



Saccadic and Postsaccadic Disconjugacy in Zebrafish Larvae Suggests Independent Eye Movement Control

Chien-Cheng Chen^{1,2}, Christopher J. Bockisch^{1,3,4*}, Dominik Straumann^{1,5,6} and Melody Ying-Yu Huang^{1,5,6}

¹ Department of Neurology, University Hospital Zurich, University of Zurich, Zurich, Switzerland, ² PhD Program in Integrative Molecular Medicine, Life Science Graduate School, University of Zurich, Zurich, Switzerland, ³ Department of Ophthalmology, University Hospital Zurich, University of Zurich, Zurich, Switzerland, ⁴ Department of Otorhinolaryngology, University Hospital Zurich, University of Zurich, Zurich, Switzerland, ⁵ Zurich Center for Integrative Human Physiology (ZIHP), University of Zurich, Zurich, Switzerland, ⁶ Neuroscience Center Zurich (ZNZ), University of Zurich and ETH Zurich, Zurich, Switzerland

Spontaneous eye movements of zebrafish larvae in the dark consist of centrifugal saccades that move the eyes from a central to an eccentric position and postsaccadic centripetal drifts. In a previous study, we showed that the fitted single-exponential time constants of the postsaccadic drifts are longer in the temporal-to-nasal (T->N) direction than in the nasal-to-temporal (N->T) direction. In the present study, we further report that saccadic peak velocities are higher and saccadic amplitudes are larger in the N->T direction than in the T->N direction. We investigated the underlying mechanism of this ocular disconjugacy in the dark with a top-down approach. A mathematic ocular motor model, including an eye plant, a set of burst neurons and a velocity-to-position neural integrator (VPNI), was built to simulate the typical larval eye movements in the dark. The modeling parameters, such as VPNI time constants, neural impulse signals generated by the burst neurons and time constants of the eye plant, were iteratively adjusted to fit the average saccadic eye movement. These simulations suggest that four pools of burst neurons and four pools of VPNI are needed to explain the disconjugate eye movements in our results. A premotor mechanism controls the synchronous timing of binocular saccades, but the pools of burst and integrator neurons in zebrafish larvae seem to be different (and maybe separate) for both eyes and horizontal directions, which leads to the observed ocular disconjugacies during saccades and postsaccadic drifts in the dark.

Keywords: ocular motor, saccades, gaze holding, brainstem, zebrafish, larvae

OPEN ACCESS

Edited by:

Lionel G. Nowak,
Brain and Cognition Research Center
(CNRS), France

Reviewed by:

Luis Herrero,
University of Seville, Spain
Jérôme Fleuriel,
University of Washington, USA

*Correspondence:

Christopher J. Bockisch
Chris.Bockisch@usz.ch

Received: 25 May 2016

Accepted: 20 September 2016

Published: 05 October 2016

Citation:

Chen C-C, Bockisch CJ,
Straumann D and Huang MY-Y
(2016) Saccadic and Postsaccadic
Disconjugacy in Zebrafish Larvae
Suggests Independent Eye
Movement Control.
Front. Syst. Neurosci. 10:80.
doi: 10.3389/fnsys.2016.00080

INTRODUCTION

Many lateral-eyed afoveate animals, such as rabbit (Collewyn, 1969; Baarsma and Collewyn, 1974), rat (Hess et al., 1985; van Alphen et al., 2010), goldfish (Easter, 1971; Beck et al., 2004), and zebrafish (Beck et al., 2004; Huang and Neuhaus, 2008), display yoked eye movements: the two eyes move in the same direction and the timings of binocular saccades

Abbreviations: VPNI, Velocity-to-position neural integrator; N->T, Nasal-to-temporal; T->N, Temporal-to nasal.

are synchronous. Such yoked eye movements help to maintain the spatial relationship between the two visual fields (Voss and Bischof, 2009) as well as to estimate self-motion with respect to the world (Nakayama, 1985; Koenderink, 1986).

Previously it has been shown that, in the dark, 5 days post fertilization (dpf) zebrafish larvae display spontaneous eye movements consisting of centrifugal saccades and subsequent postsaccadic centripetal drifts (see typical eye traces in Figure 1 of Chen et al., 2014). Although the saccade onsets and the directions were consistent in both eyes, the eye drifting in the nasal-to-temporal (N->T) direction moved faster than the eye drifting in the temporal-to-nasal (T->N) direction. Thus, the average time constants of drift (single exponential fits) were 1.8 s in the N->T direction and 3.8 s in the T->N direction (Chen et al., 2014). Since the drifts of the two eyes were disconjugate, it is conceivable that such disconjugacy may also exist in the centrifugal saccades. In the present study, we re-analyzed the data from our previous study (Chen et al., 2014) by calculating saccadic peak velocities and saccadic amplitudes. After confirming both the disconjugate saccadic and postsaccadic eye movements in our results, we raised the following question: what is the underlying mechanism responsible for the yoked but disconjugate eye movements of zebrafish larvae in the dark?

The neuroanatomy of the saccade generation and gaze holding is far better understood in primates than in zebrafish. The actions of four horizontal extraocular muscles (lateral and medial recti muscles of each eye) need to be coordinated to generate yoked horizontal saccadic eye movements (ignoring the smaller contribution of the other extraocular muscles). Excitatory burst neurons in the paramedian pontine reticular formation produce a high frequency discharge, proportional to eye velocity (van Gisbergen et al., 1981), that is sent to the ipsilateral abducens nucleus, where axons contact abducens motor neurons (MN) and internuclear neurons. The internuclear neurons project contralaterally to connect with medial rectus MNs in the oculomotor nucleus (Fuchs et al., 1988). In this way, the excitatory burst produces yoked eye movements by stimulating the ipsilateral lateral rectus and the contralateral medial rectus muscle. To inhibit the antagonistic muscle, inhibitory burst neurons in the rostral medulla project contralaterally to inhibit both MNs and interneurons in the abducens nucleus (Hikosaka et al., 1978; Strassman et al., 1986), thus relaxing both antagonistic muscles. Ocular motoneurons receive a pulse of innervation (velocity command) generated by burst neurons. This causes a phasic contraction of the extraocular muscles so the eyes quickly move to an eccentric eye position. The same pulse signal is also sent to the neural integrator cells in the nucleus prepositus hypoglossi (Cannon and Robinson, 1987; Cheron and Godaux, 1987) and medial vestibular nucleus (McFarland and Fuchs, 1992; McConville et al., 1994) that generate a step of innervation (position command) which further causes a tonic contraction of the extraocular muscles to hold the eye at its new position.

In teleost fish, the regions homologous to the primate saccadic burst generator and neural integrator have also been identified. Stimulation of a small hindbrain region in rhombomere 5 of zebrafish larvae produces binocular, ipsilaterally directed

eye movements (Schoonheim et al., 2010), consistent with the action of the saccade burst generator in primates. Likewise, the oculomotor neural integrator for horizontal eye movements has also been identified in goldfish (Pastor et al., 1994; Aksay et al., 2000, 2001).

We addressed our question by simulating spontaneous eye movements in the dark. We adopted a parsimonious ocular motor model composed of three elements (Robinson, 1964): a premotor input, simulating the eye-velocity impulse signal generated by the burst neurons (van Opstal and Goossens, 2008; van der Willigen et al., 2011); a velocity-to-position neural integrator (VPNI) that converts the impulse signal (eye velocity) to a step command (eye position) to keep gaze stable at an eccentric position (Robinson, 1964; Cohen and Komatsuzaki, 1972; Skavenski and Robinson, 1973); and an eye plant model (Keller, 1977; van Gisbergen et al., 1981). The simulated outputs, such as the saccadic peak velocity, the saccadic amplitude and the simulated postsaccadic drift, describe the behavior of eye movements in the dark. These model parameters were iteratively adjusted to fit the average saccadic eye movements of all left eyes in the N->T direction. By analyzing how the model parameters affect the simulated saccadic eye movements, we discuss the origin of the oculomotor disconjugacies in zebrafish larvae.

MATERIALS AND METHODS

Fish Maintenance and Breeding

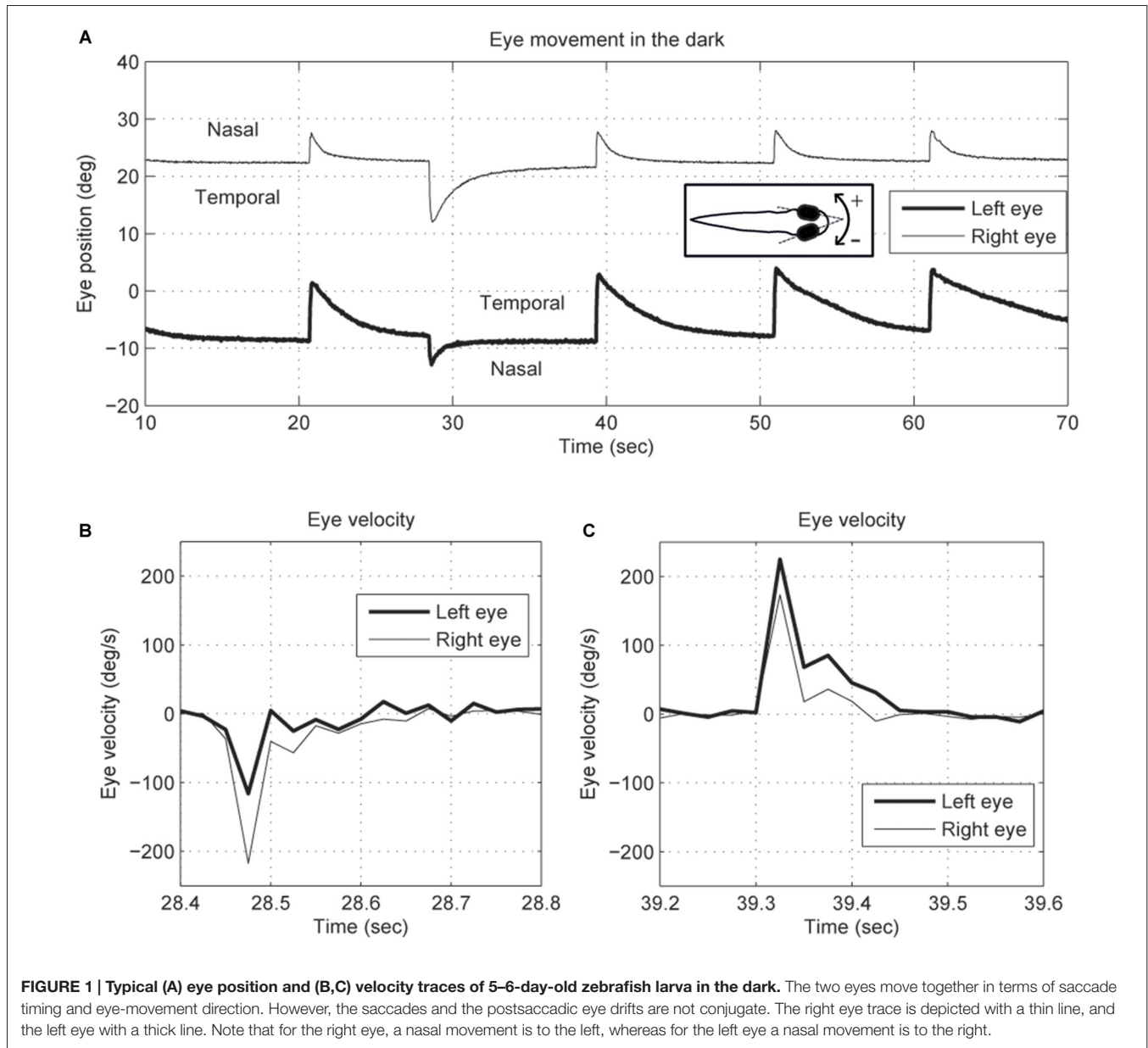
We re-analyzed the same experimental data as in the study by Chen et al. (2014). Ten 5–6 dpf zebrafish larvae were recorded, but one larva showed no left-to-right saccades. Therefore, only nine fish were studied for this direction.

Larvae were raised according to the protocol described by Mullins et al. (1994). Embryos were placed in E3 medium (5 mM NaCl, 0.17 mM KCl, 0.33 mM CaCl₂, and 0.33 mM MgSO₄) with a temperature of 28° and raised under a 10 h dark/ 14 h light cycle (Haffter et al., 1996).

All experiments were performed in accordance with the animal welfare guidelines of the Federal Veterinary Office of Switzerland. Experiments adhered to the Association for Research in Vision and Ophthalmology Statement for the Use of Animals in Ophthalmic and Vision Research.

Recording of Eye/Body Movements

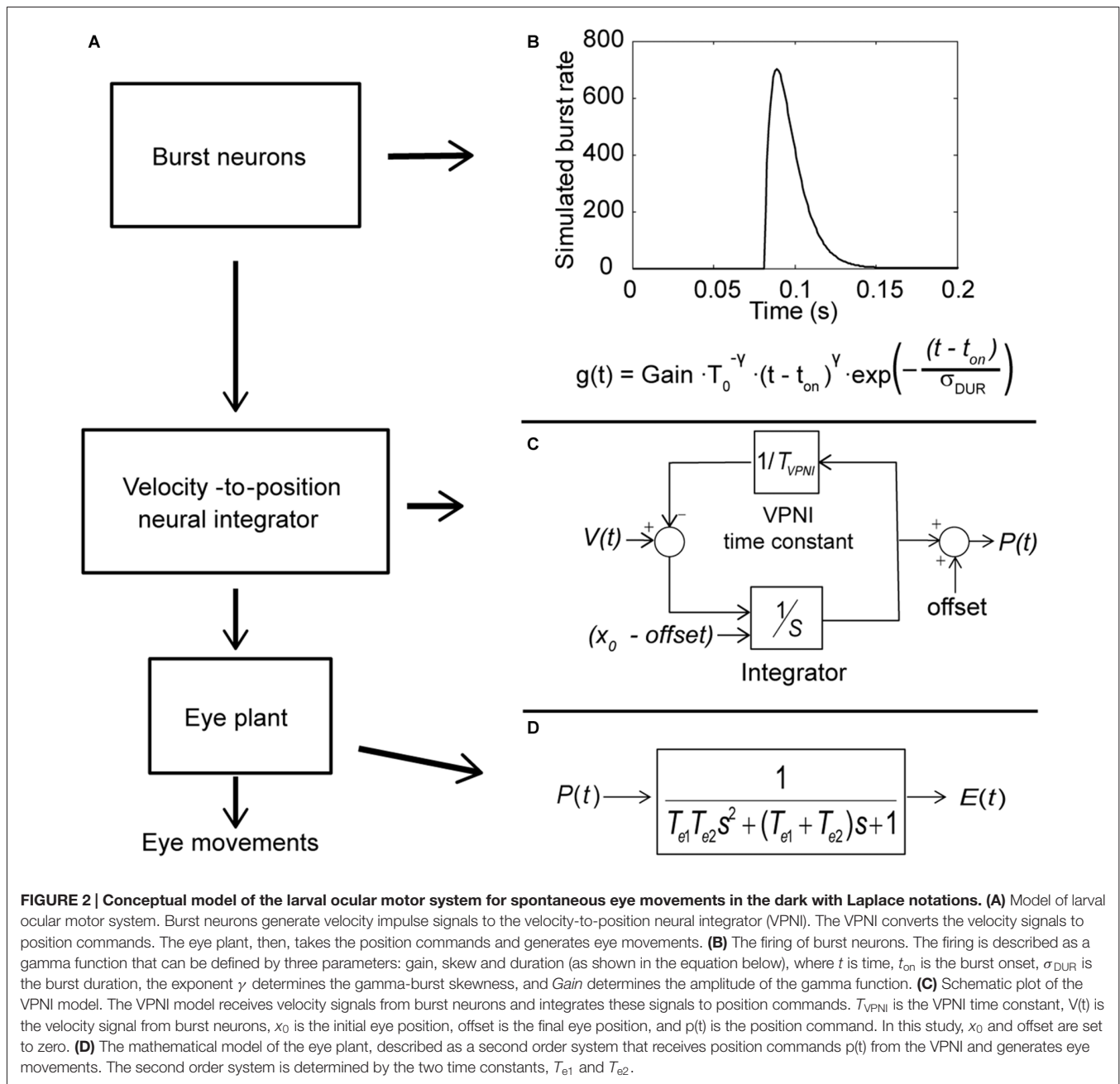
The eye and body movements of each tested larva were recorded in the dark for 10 min. In order to restrict whole-body motion without constraining eye movements, larva were placed dorsal up in a 21 mm transparent plastic tube filled with 3–3.5% methylcellulose. The plastic tube was placed on a platform where infrared emitting diodes ($\lambda_{\text{peak}} = 875 \pm 15$ nm, OIS-150 880, OSA Opto Light GmbH, Germany) illuminated the larva from below and an infrared sensitive charge-coupled device camera recorded eye and body movements at 40 frames/s from above. A custom-written program in LabVIEW (version 10.0, National Instruments, Austin, TX, USA) extracted the larval eye position in each frame. A binary threshold was used to



graphically isolate the eyes along with a user-defined region of interest, with image erosion to smooth the edges. Seen from above, the eyes are oval-shaped, so the eye orientation was determined by calculating the axis with the lowest angular momentum. The eye-position analysis was done on-line and monitored by the experimenter, while body-position analysis was done off-line by calculating the body axis in each frame with a similar image processing algorithm as used for the eye measurement. The larval body movement was used to calculate the eye movement relative to the body as well as to check the timing of body movements (typically short duration vibrations separated by long stationary intervals). All off-line analysis was written in MATLAB (Mathworks, Natick, MA, USA).

Data Analysis, Saccade Selection and Iterative Fitting Procedure

We describe eye movements according to whether they are directed nasally or temporally, so, for example, a conjugate movement to the right would be a temporal movement of the right eye and a nasal movement of the left eye. Negative rotations are to the right. Relative to the body, the eyes tend to maintain a steady position when they are rotated nasally. In **Figure 1**, for example, the right eye drifts back to about 22° , and the left eye about -9° , though these values vary between larvae. Eye-position traces were smoothed using a Gaussian smoothing kernel with a cut-off frequency of 16 Hz. Eye-velocity and acceleration were obtained from the derivatives of eye position. Since the spontaneous eye movements in zebrafish larvae usually start with



a saccade to an eccentric position followed by a drift back to a central eye position (Figure 1), the saccade selection was done by: (1) separating the eye position curve into segments based on the eye-movement direction; and (2) identifying a segment as a saccade if the maximum acceleration was $>500 \text{ deg/s}^2$. The other segments would be identified as slow eye drifts. Each eye drift was fitted with a single exponential decay curve to obtain a time constant by using the MATLAB function `nlsgnonlin.m`.

Saccadic peak velocities were obtained by calculating the maximum absolute velocity of each saccade. The start and end points of saccades were found by determining the first sample

when eye velocity reversed direction. Saccadic peak velocity to saccadic amplitude ratios were calculated in each saccade.

Statistical Analysis

Directional preferences were determined by two tests. In the first test, we separated saccades of each tested larva into two groups based on the N->T and T->N directions. Then, a t -test was done between the two groups to check whether there exists a significant difference between the two eye-movement directions.

In the second test, we further checked whether there exists a significant difference between the two eye-movement directions

of the two eyes. Thus, we separated saccades of each tested larva into four groups based on the N->T and T->N directions of the two eyes. Then the median value of each group was calculated. A binomial test was used to test the frequency that N->T saccades had a higher peak velocity (or amplitude) than T->N saccades. Since the eye movements of zebrafish larvae are yoked, a T->N movement of one eye co-occurs with an N->T movement of the other eye and vice versa. Thus, the saccadic peak velocity of the T->N movement of the left eye was compared with the one of the N->T movement of the right eye and vice versa.

Computer Simulation

Computer simulations were done in MATLAB Simulink (Mathworks, Natick, MA, USA). The model includes three subsystems: a set of burst neurons, a VPNI and an eye plant (see **Figure 2A**). Conceptually, the burst neurons generate eye-velocity impulse signals to quickly change the eye position. Previous studies described such velocity impulse signals as a gamma function (see **Figure 2B**; van Opstal and Goossens, 2008; van der Willigen et al., 2011):

$$g(t) = \text{Gain} \cdot T_0^{-\gamma} \cdot (t - t_{\text{on}})^{\gamma} \cdot \exp\left(-\frac{(t - t_{\text{on}})}{\sigma_{\text{DUR}}}\right)$$

where t is time, t_{on} is the burst onset, σ_{DUR} is the burst duration, $T_0 = \sigma_{\text{DUR}} \gamma/e$ and $t \geq t_0$. The exponent γ determines the gamma-burst skewness, and *Gain* determines the amplitude of the gamma function.

The VPNI converts the eye-velocity impulse signals to eye-position commands. A previous study found that the VPNI in zebrafish larvae is leaky (Miri et al., 2011). Such a leaky VPNI can be modeled by using an integrator with a single time constant as shown in **Figure 2C** (Chen et al., 2014). These eye-position commands are sent to the eye plant to generate the simulated eye movements. The eye plant in the monkey has been described as a second order system assembled by two time constants T_{e1} and T_{e2} , shown in **Figure 2D** (Keller, 1977; van Gisbergen et al.,

1981). Note that the equivalent studies in fish have not been done, but we assume the results would be similar. T_{e1} is approximately equal to the ratio of the viscous drag and the elastic stiffness of the orbital tissues while T_{e2} is approximately equal to the ratio of mass of the eye ball and the viscous drag of the orbital tissues. In general, T_{e1} is much larger than T_{e2} since the mass of the eye is relatively small compared to the effect of the elastic stiffness and the viscous drag of the orbital tissues. For instance, in the model of van Gisbergen et al. (1981) for monkey, T_{e1} and T_{e2} were set to 0.15 and 0.004, respectively. In this study, we used the product of the two time constants ($T_{e1} \times T_{e2}$), which refers to the ratio of mass of the eye ball and the elastic stiffness of the orbital tissues, and the sum of two time constants ($T_{e1} + T_{e2}$), which represents the ratio of the viscous drag and the elastic stiffness of the orbital tissues. Since T_{e1} is much larger than T_{e2} , the sum of T_{e1} and T_{e2} is much larger than the product of T_{e1} and T_{e2} .

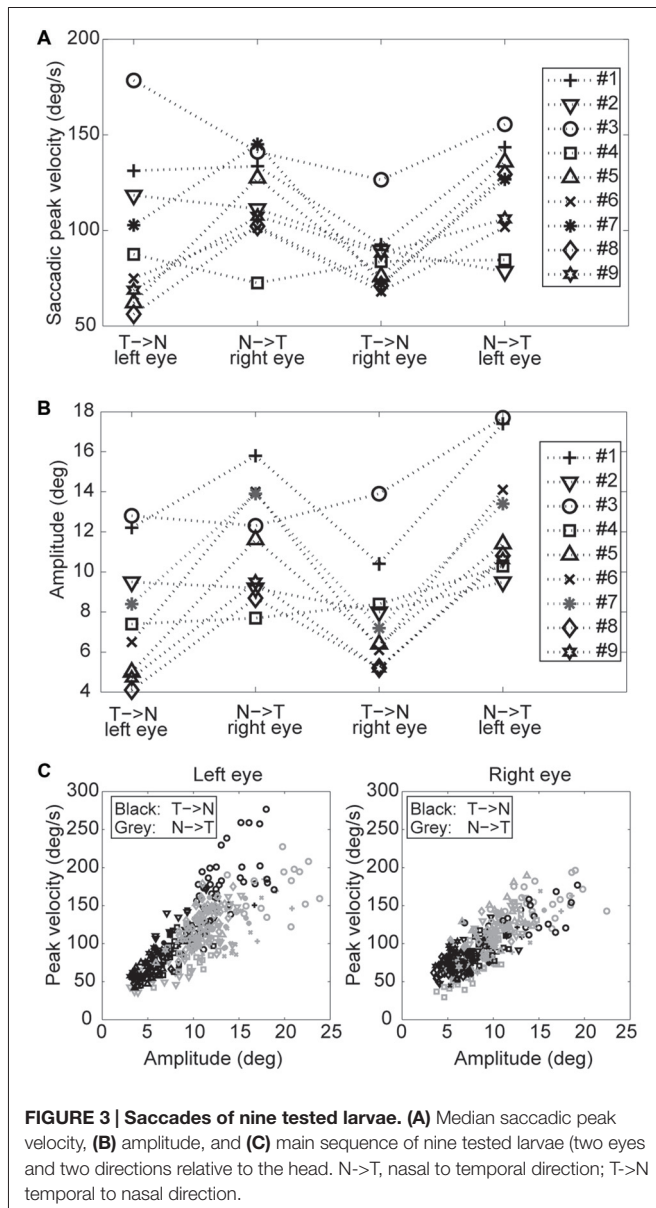
RESULTS

Spontaneous Eye Movements in the Dark

An example of the pattern of centrifugal saccades and centripetal drifts is depicted in **Figure 1**. Clearly, the centrifugal saccades of both eyes were disconjugate. **Table 1** lists the median saccadic peak velocity, the median saccadic amplitude and the median ratio of each larva (also see **Figure 3**). The main sequence is also plotted to visualize the variation between eye-movement directions and larvae (see **Figure 3C**). Since the medium used to restrain body movements could also affect the eye movement recording, our results can be compared to those by Beck et al. (2004), who restricted only the body movement with agarose. In this measuring method with a higher recording frame rate (60 Hz), the slopes of maximum velocity vs. amplitude (in our case, we use the term “ratio”) in zebrafish larvae were 12–13 (Beck et al., 2004, Figure 5B), which are similar to values in our study (see **Table 1**, Ratio). Moreover, another study Ma et al. (2014) showed that 5-

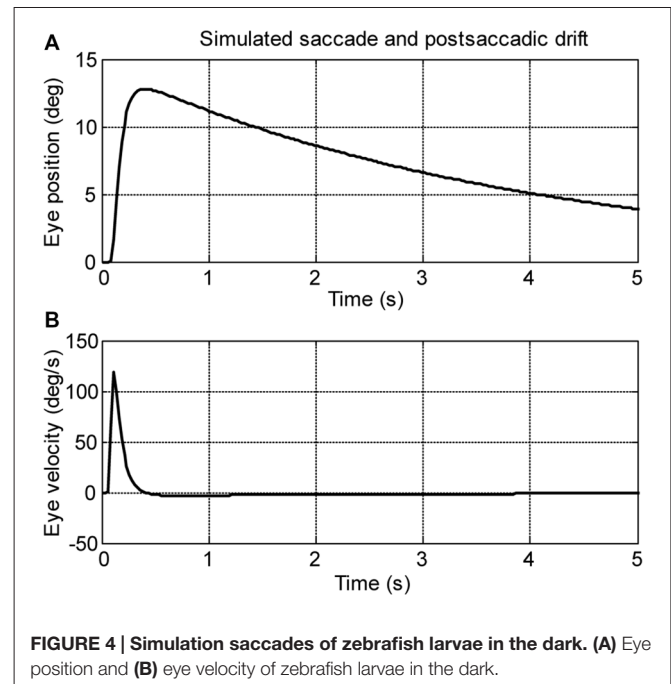
TABLE 1 | Saccadic peak velocity, saccadic amplitude and the ratio in eyes and eye-movement directions.

Subject	Left eye								Right eye							
	Peak velocity		Amplitude		Ratio		Number		Peak velocity		Amplitude		Ratio		Number	
	T-N	N-T	T-N	N-T	T-N	N-T	T-N	N-T	T-N	N-T	T-N	N-T	T-N	N-T	T-N	N-T
1	131.2	143.5	12.2	17.4	10.4	8.4	4	6	92.6	133.6	10.4	15.8	9.5	8.5	6	4
2	118.4	78.5	9.5	9.5	13.2	9.1	23	25	89.6	111.3	8.0	9.2	11.6	12.5	25	23
3	178.5	155.5	12.8	17.7	13.8	9.4	35	20	126.5	141.1	13.9	12.3	9.8	10.9	20	35
4	87.5	84.6	7.4	10.3	11.8	8.6	51	23	83.7	72.5	8.4	7.7	9.7	9.4	23	51
5	62.1	135.8	5.0	11.4	12.4	12.0	23	6	75.9	127.4	6.4	11.6	12.9	11.6	6	23
6	74.9	101.8	6.5	14.1	11.6	8.0	3	17	68.0	101.3	6.1	14.0	11.0	8.3	17	3
7	102.8	126.7	8.4	13.4	12.7	9.1	2	11	72.1	145.1	7.2	13.9	10.5	10.6	11	2
8	56.2	129.3	4.1	10.8	13.4	12.1	10	50	71.1	102.2	5.2	8.7	14.0	12.2	50	10
9	68.7	106.0	4.7	10.6	17.0	10.5	13	9	88.1	107.4	5.2	9.5	16.1	11.1	9	13
Mean	97.8	118.0	7.8	12.8	12.9	9.7	–	–	85.3	115.8	7.9	11.4	11.7	10.6	–	–
STD	39.6	26.6	3.2	3.1	1.8	1.5	–	–	17.8	23.2	2.8	2.8	2.3	1.5	–	–



dpf wild type zebrafish larvae had an average saccadic peak velocity of about $137^\circ/s$ with a 200 Hz framerate, which is similar to our results. In the same study, the disconjugacy can be found in fast phase velocity during optokinetic stimulation.

Using a one-tail *t*-test, we found that the saccadic amplitudes were significantly larger ($p < 0.05$) for saccades in the N->T direction than those in the T->N direction in eight of nine tested larvae, while the saccadic peak velocities were significantly higher ($p < 0.05$) for saccades in the N->T direction than those in the T->N direction in six of nine tested larvae. All non-significant *p*-values were < 0.1 . Using a binomial test with 18 pairs (since there are two pairs (a T->N movement of one eye co-occurs with a N->T movement of the other eye and vice versa) in one fish, there are 18 pairs in this test), we found that both the median



saccadic peak velocities and the median saccadic amplitudes were larger in the N->T direction than those in the T->N direction (for peak velocity, $n = 18$, $Z = 2.36$, $p = 0.0091$; for amplitude, $n = 18$, $Z = 2.83$, $p = 0.0023$).

Postsaccadic exponential centripetal drifts were disconjugate, as we demonstrated previously (Chen et al., 2014; **Figure 2D**).

Simulation of Spontaneous Eye Movements in the Dark

A computational model (see **Figure 2**) was used to simulate larval eye movements in the dark. The model parameters were iteratively adjusted to fit the average median saccade in the N->T direction and the average median eye-drift time constant in the T->N direction of the left eyes. **Figure 4** shows the simulated eye movements. The model parameters resulting from the iterative fitting were used for the simulation and are listed and highlighted in gray at the top of **Table 2** while the simulated saccade and postsaccadic eye drift in the dark are listed and highlighted in gray at the bottom of **Table 2**.

In order to study how changes of single model parameters affect the simulated outputs, we first increased each parameter by 10% of its original value (see **Table 2**, top) to record the corresponding changes in the model outputs (see **Table 2**, bottom).

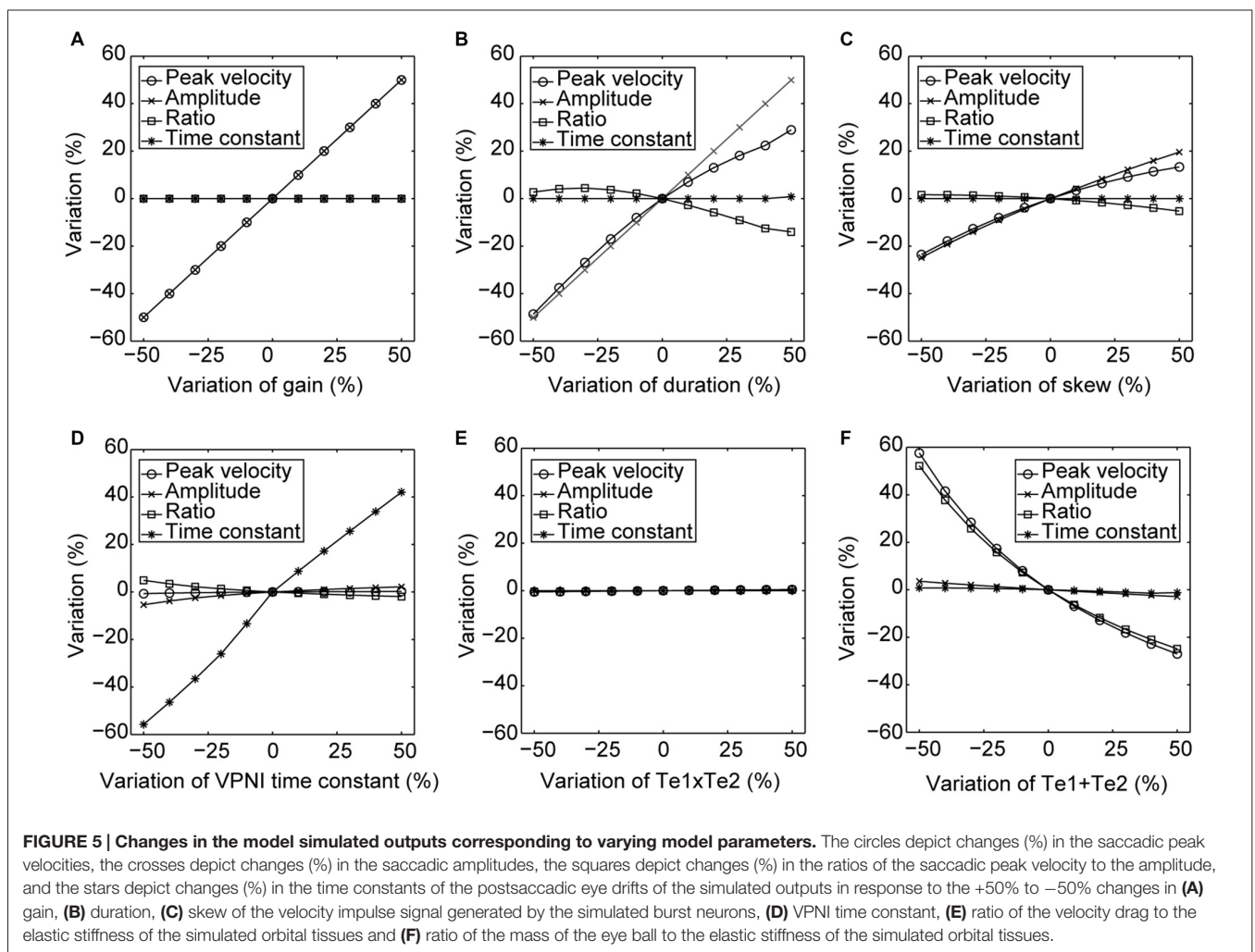
For the burst neuron related parameters, the simulation shows that a 10% increase in *gain* and *duration* has a direct impact on the saccadic peak velocity and amplitude (change $\geq 7\%$), but much less on the saccadic peak velocity to amplitude ratio (change $\leq 3\%$). The postsaccadic eye drift time constant (*T*), on the other hand, is barely affected (change $< 1\%$). A 10% increase in skew has a low impact on the simulated outputs (change $\leq 4\%$).

TABLE 2 | Model parameter analysis.

Modeling parameters								
Burst neurons (Gamma distribution)	Gain	490	10%					
	Duration	0.01		10%				
	Skew	1.1			10%			
VPNI	T_{VPNI}	3.8				10%		
Eye plant	$T_{e1} + T_{e2}$	0.078					10%	
	$T_{e1}T_{e2}$	0.0001						10%
Simulated eye movements in the dark								
Saccades	Peak velocity	118	10%	7%	3%	0%	-7%	0%
	Amplitude	12.8	10%	10%	4%	1%	-1%	0%
Ratio (Peak velocity/Amplitude)		9.1	0%	-3%	-1%	-1%	-6%	0%
Eye drift	T	3.8	0%	0%	0%	10%	0%	0%

The top of the table indicates the values of the model parameters. The values in gray were obtained by iteratively fitting the empirical data. The bottom of the table shows the simulated outputs and elucidates how each model parameter affects the simulated saccade and postsaccadic drift.

For the VPNI related parameters, a 10% increase in VPNI time constant mainly affects the simulated postsaccadic centripetal drift (change = 10%). The effect on the simulated centrifugal saccade is minimal (change $\leq 1\%$).



For the eye-plant related parameters, a 10% increase of $T_{e1} + T_{e2}$ (referring to the ratio of the viscous drag to the elastic stiffness of orbital tissues) lowers the simulated saccadic peak velocity by 7%, the ratio of saccadic peak velocity to amplitude by 6%, but the saccadic amplitude only by 1%. The simulated postsaccadic eye drift is not affected by this change. A 10% increase of $T_{e1} \times T_{e2}$ (referring to the ratio of the mass of the eye ball to the elastic stiffness of orbital tissues) has little or no influence on the simulated outputs (all changes are below 1%).

Furthermore, to better visualize the dependency of the simulated output on each single model parameter, **Figure 5** demonstrates simulated outputs of the model in response to variations of each of the six model parameters within a range from -50% to $+50\%$. The simulation results lead to similar conclusions as indicated in **Table 2**: simulated saccadic velocities and amplitudes are mainly affected by parameters related to the burst neurons, while the simulated postsaccadic eye drifts are mostly determined by the VPNI time constant.

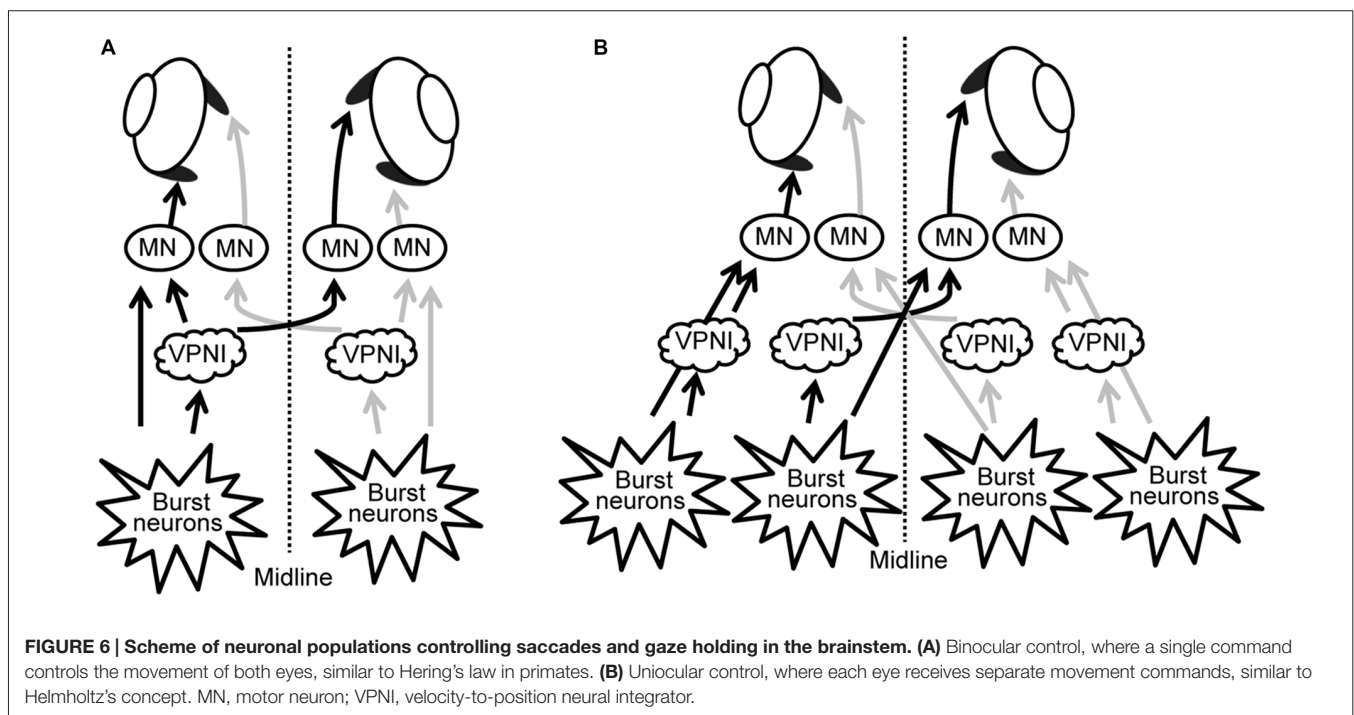
DISCUSSION

Saccadic and Postsaccadic Disconjugacy in Zebrafish Larvae in Dark

In this study, we investigated the disconjugacy of spontaneous horizontal eye movements of zebrafish larvae in the dark. Typical eye movements of larvae in the dark consist of spontaneous centrifugal saccades that move the eyes eccentrically and subsequent centripetal eye drifts that bring the eyes back toward the center (see **Figure 1**). Although both eyes moved in the same direction and are synchronized, the two eye movements

were shown to be disconjugate. The saccadic peak velocities were higher and amplitudes were significantly larger in the (N->T) direction than in the (T->N) direction (**Figure 3**), while the fitted single-exponential time constants of postsaccadic eye drifts were significantly longer in the T->N direction than in the N->T direction. Such a disconjugate eye movement cannot be due to the mechanical limit of the orbit. In our previous study (Chen et al., 2014), we found that spontaneous saccades in zebrafish larvae occurred mainly in the central area of the eye-movement range. For instance, **Figure 4A** in our previous study (Chen et al., 2014) is a typical eye movement example in zebrafish larvae. The spontaneous saccades mainly existed in a range of $5\text{--}20^\circ$ of the right eye; the mechanical limit, however, ranges from -5° to 35° . Moreover, as we mentioned in Chen et al. (2014), the VPNI is leaky in zebrafish larvae so that their eyes drift back to a central area after saccades. Thus, to our observation, it is rare that saccades occur in an eccentric area and reach the mechanical limit of the orbit. We also observed a large variation in the saccadic peak velocities among the tested larvae. It could be that the neural and muscular systems of 5–6 dpf larvae have not fully developed. Therefore, some larvae had a strong ocular motor response while others do not.

We further studied the disconjugate eye movements with a top-down approach to identify possible causes for this disconjugacy: a computational ocular motor model composed of burst neurons, a VPNI, and an eye plant was adopted to simulate eye movements in zebrafish larvae in the dark (see **Figure 2**). After adjusting the model parameters to fit the average N->T centrifugal saccade and the average T->N centripetal postsaccadic eye drift of left larval eyes, we varied each parameter separately to see how changes in single model parameters affect the simulated output. Our results (see **Table 2** and **Figure 5**)



showed that the simulated saccadic amplitude is mainly changed by the firing properties of the saccadic burst neurons, which suggests that the observed different saccadic amplitudes in the N->T and T->N directions of the two eyes (see **Figure 3**) may be attributed to unmatched firings of burst neurons for each eye and for each direction. The simulated saccadic peak velocity, on the other hand, is influenced by both firing properties of burst neurons and the ratio of the viscous drag to the elastic stiffness of the orbital tissues. It is conceivable that the viscosity of the orbital tissues has a direct impact on eye velocities. Thus, an increased ratio of the viscous drag to the elastic stiffness would lower the saccadic peak velocity and therefore change as well the ratio of saccadic peak velocity to the amplitude. In our model, the ratio of the mass of the eye ball to the elastic stiffness of orbital tissues has no influence on the simulated eye movements, which implies that the inertia of the eye should not be responsible for the disconjugate eye movements as its effect is likely too small. The simulated postsaccadic centripetal eye drifts are mainly determined by the VPNI time constant. This suggests that for each eye there exist two distinct neural populations of VPNI, i.e., a total of four neural populations. Only such a configuration can account for different eye drift time constants in N->T and T->N directions of the two eyes.

Eye Movement Control

How exactly an ocular motor network controls yoked eye movements has been debated for decades. Two controversial hypotheses of binocular coordination were raised back in the 19th century by the eminent German physiologists, Hermann von Helmholtz and Ewald Hering. While von Helmholtz (1962) argued that the movement control of the two eyes is independent and thus binocular coordination is a learned behavior, Hering (1977) stated that the binocular coordination is an inborn behavior and that two eyes do not move separately but rather the same impulse will direct both eyes to move simultaneously. Subsequently, the latter hypothesis, known as Hering's Law of Equal Innervation, has generally been favored (Howard and Rogers, 1996); however, both theories have been supported for a variety of reasons and by substantial evidence (for review see King and Zhou, 2000).

Our results suggest that, rather than having a single unique control system for both eyes, the two eyes of zebrafish are controlled independently by distinct neuronal populations (see **Figures 6A,B**). These, in turn, are driven by premotor mechanisms that ensure synchronous timing of binocular saccades in the same horizontal direction.

REFERENCES

- Aksay, E., Baker, R., Seung, H. S., and Tank, D. W. (2000). Anatomy and discharge properties of pre-motor neurons in the goldfish medulla that have eye-position signals during fixations. *J. Neurophysiol.* 84, 1035–1049.
- Aksay, E., Gamkrelidze, G., Seung, H. S., Baker, R., and Tank, D. W. (2001). *In vivo* intracellular recording and perturbation of persistent activity in a neural integrator. *Nat. Neurosci.* 4, 184–193. doi: 10.1038/84023
- Baarsma, E. A., and Collewijn, H. (1974). Vestibulo-ocular and optokinetic reactions to rotation and their interaction in the rabbit. *J. Physiol.* 238, 603–625. doi: 10.1113/jphysiol.1974.sp010546
- Beck, J. C., Gilland, E., Tank, D. W., and Baker, R. (2004). Quantifying the ontogeny of optokinetic and vestibuloocular behaviors in zebrafish, medaka and goldfish. *J. Neurophysiol.* 92, 3546–3561. doi: 10.1152/jn.00311.2004
- Cannon, S. C., and Robinson, D. A. (1987). Loss of the neural integrator of the oculomotor system from brain stem lesions in monkey. *J. Neurophysiol.* 57, 1383–1409.

Evidence in primates has led to a similar conclusion. Premotor neurons have been found which preferentially encode the movement or position of one eye (King and Zhou, 2000; Sylvestre et al., 2003; Van Horn and Cullen, 2008; Van Horn et al., 2008; Waitzman et al., 2008). In particular, excitatory burst neurons have been identified which encode monocular saccade velocity, rather than a conjugate command (King and Zhou, 2000), and neurons that are part of the VPNI generally encode the position of only one eye during disjunctive movements (Sylvestre et al., 2003).

The debate between Hering and von Helmholtz concerned primate eye movements, who, being frontal eyed and foveate, have a greater demand for precise synchronization of the movement of both eyes compared to lateral eyed fish. Since the oculomotor system should be able to adapt to changes due to aging and disease, it would be reasonable for eye alignment to be under adaptive control. Recording (Walton and Mustari, 2015) and microstimulation studies (Walton et al., 2013) of the monkey saccade burst generating regions in strabismic monkeys shows that these structures are altered compared to non-strabismic monkeys. These authors suggested that the premotor neurons have binocular connections, though the strength of these connections can be altered, so pools of premotor neurons could be predominately monocular. Our results suggest a similar situation could exist in zebrafish, adding further support for the use of this species as a model for understanding the oculomotor system in primates (Joshua and Lisberger, 2015).

AUTHOR CONTRIBUTIONS

DS, C-CC and MY-YH conceived the study. C-CC performed the experiments. C-CC, DS, CJB, and MY-YH analyzed the data. C-CC, DS, CJB, and MY-YH drafted the article. All authors approved the final version of the article.

ACKNOWLEDGMENTS

The authors would like to thank Prof. Stephan Neuhaus for providing the fish larvae and for advice in conducting animal experiments, Marco Penner for technical assistance, Kara Dannenhauer for fish care, and Giovanni Bertolini for helpful discussions about the data. This work was supported by the Swiss National Science Foundation (SNF) grants #139754 (Marie Heim-Vögtlin programme) and #149521, the Betty and David Koetser Foundation for Brain Research, and the Dr. Dabbous Foundation.

- Chen, C. C., Bockisch, C. J., Bertolini, G., Olasagasti, I., Neuhaus, S. C., Weber, K. P., et al. (2014). Velocity storage mechanism in zebrafish larvae. *J. Physiol.* 592, 203–214. doi: 10.1113/jphysiol.2013.258640
- Cheron, G., and Godaux, E. (1987). Disabling of the oculomotor neural integrator by kainic acid injections in the prepositus-vestibular complex of the cat. *J. Physiol.* 394, 267–290. doi: 10.1113/jphysiol.1987.sp016870
- Cohen, B., and Komatsuzaki, A. (1972). Eye movements induced by stimulation of the pontine reticular formation: evidence for integration in oculomotor pathways. *Exp. Neurol.* 36, 101–117. doi: 10.1016/0014-4886(72)90139-2
- Collewijn, H. (1969). Optokinetic eye movements in the rabbit: input-output relations. *Vision Res.* 9, 117–132. doi: 10.1016/0042-6989(69)90035-2
- Easter, S. S. (1971). Spontaneous eye movements in restrained goldfish. *Vision Res.* 11, 333–342. doi: 10.1016/0042-6989(71)90244-6
- Fuchs, A. F., Scudder, C. A., and Kaneko, C. R. S. (1988). Discharge patterns and recruitment order of identified motoneurons and internuclear neurons in the monkey abducens nucleus. *J. Neurophysiol.* 60, 1874–1895.
- Haffter, P., Granato, M., Brand, M., Mullins, M. C., Hammerschmidt, M., Kane, D. A., et al. (1996). The identification of genes with unique and essential functions in the development of the zebrafish, *Danio rerio*. *Development* 123, 1–36.
- Hering, E. (1977). *The Theory of Binocular Vision*. New York, NY: Plenum Press.
- Hess, B. J. M., Prechta, W., Reber, A., and Cazin, L. (1985). Horizontal optokinetic ocular nystagmus in the pigmented rat. *Neuroscience* 15, 97–107. doi: 10.1016/0306-4522(85)90126-5
- Hikosaka, O., Igusa, Y., Nakao, S., and Shimazu, H. (1978). Direct inhibitory synaptic linkage of pontomedullary reticular burst neurons with abducens motoneurons in the cat. *Exp. Brain Res.* 33, 337–352. doi: 10.1007/bf00235558
- Howard, I. P., and Rogers, B. J. (1996). *Binocular Vision and Stereopsis*. New York, NY: Oxford University Press, 736.
- Huang, Y. Y., and Neuhaus, S. C. F. (2008). The optokinetic response in zebrafish and its applications. *Front. Biosci.* 13, 1899–1916. doi: 10.2741/2810
- Joshua, M., and Lisberger, S. G. (2015). A tale of two species: neural integration in zebrafish and monkeys. *Neuroscience* 296, 80–91. doi: 10.1016/j.neuroscience.2014.04.048
- Keller, E. L. (1977). “Control of saccadic eye movements by midline brain stem neurons,” in *Control of Gaze by Brain Stem Neurons*, eds R. Baker and A. Berthoz (Amsterdam: Elsevier), 327–336.
- King, W. M., and Zhou, W. (2000). New ideas about binocular coordination of eye movements: is there a chameleon in the primate family tree? *Anat. Rec.* 261, 153–161. doi: 10.1002/1097-0185(20000815)261:4<153::AID-AR4>3.0.CO;2-4
- Koenderink, J. J. (1986). Optic flow. *Vision Res.* 26, 161–179. doi: 10.1016/0042-6989(86)90078-7
- Ma, L. H., Grove, C. L., and Baker, R. (2014). Development of oculomotor circuitry independent of hox3 genes. *Nat. Commun.* 5:4221. doi: 10.1038/ncomms5221
- McConville, K., Tomlinson, R. D., King, W. M., Paige, G., and Na, E. Q. (1994). Eye position signals in the vestibular nuclei: consequences for models of integrator function. *J. Vestib. Res.* 4, 391–400.
- McFarland, J. L., and Fuchs, A. F. (1992). Discharge patterns in nucleus prepositus hypoglossi and adjacent medial vestibular nucleus during horizontal eye movement in behaving macaques. *J. Neurophysiol.* 68, 319–332.
- Miri, A., Daie, K., Arrenberg, A. B., Baier, H., Aksay, E., and Tank, D. W. (2011). Spatial gradients and multidimensional dynamics in a neural integrator circuit. *Nat. Neurosci.* 14, 1150–1159. doi: 10.1038/nn.2888
- Mullins, M. C., Hammerschmidt, M., Haffter, P., and Nüsslein-Volhard, C. (1994). Large-scale mutagenesis in the zebrafish: in search of genes controlling development in a vertebrate. *Curr. Biol.* 4, 189–202. doi: 10.1016/S0960-9822(00)00048-8
- Nakayama, K. (1985). Biological image processing: a review. *Vision Res.* 25, 625–660. doi: 10.1016/0042-6989(85)90171-3
- Pastor, A. M., De la Cruz, R. R., and Baker, R. (1994). Eye position and eye velocity integrators reside in separate brainstem nuclei. *Proc. Natl. Acad. Sci. U S A* 91, 807–811. doi: 10.1073/pnas.91.2.807
- Robinson, D. A. (1964). The mechanics of human saccadic eye movement. *J. Physiol.* 174, 245–264. doi: 10.1113/jphysiol.1964.sp007485
- Schoonheim, P. J., Arrenberg, A. B., Del Bene, F., and Baier, H. (2010). Optogenetic localization and genetic perturbation of saccade-generating neurons in zebrafish. *J. Neurosci.* 30, 7111–7120. doi: 10.1523/JNEUROSCI.5193-09.2010
- Skavenski, A. A., and Robinson, D. A. (1973). Role of abducens neurons in vestibuloocular reflex. *J. Neurophysiol.* 36, 724–738.
- Strassman, A., Highstein, S. M., and McCrea, R. A. (1986). Anatomy and physiology of saccadic burst neurons in the alert squirrel monkey. II. Inhibitory burst neurons. *J. Comp. Neurol.* 249, 358–380. doi: 10.1002/cne.902490304
- Sylvestre, P. A., Choi, J. T. L., and Cullen, K. E. (2003). Discharge dynamics of oculomotor neural integrator neurons during conjugate and disjunctive saccades and fixation. *J. Neurophysiol.* 90, 739–754. doi: 10.1152/jn.00123.2003
- van Alphen, B., Winkelman, B. H. J., and Frens, M. A. (2010). Three-dimensional optokinetic eye movements in the C57BL/6J mouse. *Invest. Ophthalmol. Vis. Sci.* 51, 623–630. doi: 10.1167/iovs.09-4072
- van der Willigen, R. F., Goossens, H. H. L. M., and van Opstal, A. J. (2011). Linear visuomotor transformations in midbrain superior colliculus control saccadic eye-movements. *J. Integr. Neurosci.* 10, 277–301. doi: 10.1142/s0219635211002750
- van Gisbergen, J. A. M., Robinson, D. A., and Gielen, S. T. A. N. (1981). A quantitative analysis of generation of saccadic eye movements by burst neurons. *J. Neurophysiol.* 45, 417–442.
- Van Horn, M. R., and Cullen, K. E. (2008). Dynamic coding of vertical facilitated vergence by premotor saccadic burst neurons. *J. Neurophysiol.* 100, 1967–1982. doi: 10.1152/jn.90580.2008
- Van Horn, M. R., Sylvestre, P. A., and Cullen, K. E. (2008). The brain stem saccadic burst generator encodes gaze in three-dimensional space. *J. Neurophysiol.* 99, 2602–2616. doi: 10.1152/jn.01379.2007
- van Opstal, A. J., and Goossens, H. H. L. M. (2008). Linear ensemble-coding in midbrain superior colliculus specifies the saccade kinematics. *Biol. Cybern.* 98, 561–577. doi: 10.1007/s00422-008-0219-z
- von Helmholtz, H. (1962). *Helmholtz's Treatise on Physiological Optics (Vol. 33)*. New York, NY: Dover Publication, Inc.
- Voss, J., and Bischof, H. J. (2009). Eye movements of laterally eyed birds are not independent. *J. Exp. Biol.* 212, 1568–1575. doi: 10.1242/jeb.024950
- Waizman, D. M., Van Horn, M. R., and Cullen, K. E. (2008). Neuronal evidence for individual eye control in the primate cMRF. *Prog. Brain Res.* 171, 143–150. doi: 10.1016/S0079-6123(08)00619-5
- Walton, M. M. G., and Mustari, M. J. (2015). Abnormal tuning of saccade-related cells in pontine reticular formation of strabismic monkeys. *J. Neurophysiol.* 114, 857–868. doi: 10.1152/jn.00238.2015
- Walton, M. M. G., Ono, S., and Mustari, M. J. (2013). Stimulation of pontine reticular formation in monkeys with strabismus. *Invest. Ophthalmol. Vis. Sci.* 54, 7125–7136. doi: 10.1167/iovs.13-12924

Conflict of Interest Statement: The authors declare that the research was conducted in the absence of any commercial or financial relationships that could be construed as a potential conflict of interest.

Copyright © 2016 Chen, Bockisch, Straumann and Huang. This is an open-access article distributed under the terms of the Creative Commons Attribution License (CC BY). The use, distribution and reproduction in other forums is permitted, provided the original author(s) or licensor are credited and that the original publication in this journal is cited, in accordance with accepted academic practice. No use, distribution or reproduction is permitted which does not comply with these terms.